Formation of Platinum-Free Fuel Cell Cathode Catalyst with Highly Developed Nanospace by Carbonizing Catalase

Jun Maruyama* and Ikuo Abe

Environmental Technology Department, Osaka Municipal Technical Research Institute, 1-6-50, Morinomiya, Joto-ku, Osaka 536-8553, Japan

Received November 24, 2004. Revised Manuscript Received June 9, 2005

The amount of platinum in the catalyst for the electrodes of polymer electrolyte fuel cells must be minimized to widely substitute this new energy system for conventional ones. In this study, a platinum-free catalyst for the cathodic oxygen reduction was formed from a natural organic compound, catalase. We carbonized catalase to produce a catalyst active in the superacidic atmosphere of the polymer electrolyte. Nitrogen adsorption onto the carbonized material revealed that the material had highly developed internal nanospaces, which were essential for exposing active sites to oxygen reduction on the pore surface. The carbonized material was also characterized by X-ray photoelectron spectroscopy, X-ray diffraction, transmission electron microscopy, and Mössbauer spectroscopy. The activity for oxygen reduction was evaluated using rotating disk electrodes, forming a catalyst layer from the carbonized material and the polymer electrolyte on the electrode surface and immersing the layer in oxygen-saturated perchloric acid. The activity increased with the increase in the specific surface area and possibly the increase in the activity of the respective active sites. A preliminary fuel cell test using the material in the cathode confirmed the electricity generation, although the performance was inferior to a Pt-based fuel cell.

Introduction

The practical use of the polymer electrolyte fuel cell (PEFC) has just recently started or will soon start as a power source of electric vehicles or a cogeneration system for domestic electricity and heating. The PEFC generates electricity by converting chemical energy to electrical energy as H_2 oxidation (reaction 1) and O_2 reduction (reaction 2) occur at the anode and the cathode, respectively.[1−4]

$$H_2 \rightarrow 2H^+ + 2e^- \quad (1)$$

$$O_2 + 4H^+ + 4e^- \rightarrow 2H_2O \quad (2)$$

Catalysts in the electrodes play a crucial role in the energy conversion as the electrode reactions occur on them, especially for the cathode because of the slow reaction rate of O_2 reduction. Nanoparticles of Pt or Pt alloys supported on electron-conductive carbon black have hitherto been used as the catalyst since it has been generally recognized that only these metals are active for the reactions and stable in the superacidic atmosphere of the polymer electrolyte, i.e., perfluorosulfonate ion-exchange membranes. The carbon black support is also essential for achieving a high performance by the PEFC. It was reported that PEFC performance was significantly improved by the efficient utilization of dispersed Pt supported on carbon black rather than platinum black in the electrodes.[5,6] Recently, catalysts have been prepared using newly developed nanosized carbon materials as the supports of Pt, such as carbon nanotubes,[7,8] carbon nanohorns,[9] and carbon nanofibers,[10−12] aimed at a further performance improvement. Nevertheless, the limited Pt reserves and supply will prohibit widespread use of the PEFC. There is accordingly demand for a catalyst that functions with far less or no Pt.

It has been demonstrated in many studies that organic macrocycles such as porphyrins and phthalocyanines adsorbed on a carbon support, coordinating Fe through four central N atoms, are active for O_2 reduction.[13,14] Iron is rich in its resource, in contrast to Pt. It has been also demonstrated

* To whom correspondence should be addressed. E-mail: maruyama@omtri.city.osaka.jp. Tel: +81-6-6963-8043. Fax: +81-6-6963-8049.

(1) Dhar, H. P. *J. Electroanal. Chem.* **1993**, *357*, 237.
(2) Appleby, A. J.; Foulkes, F. R. *Fuel Cell Handbook*; Van Nostrand Reinhold: New York, 1989.
(3) Costamagna, P.; Srinivasan, S. *J. Power Sources* **2001**, *102*, 242.
(4) Gottesfeld, S.; Zawodzinski, T. A. In *Advances in Electrochemical Science and Engineering*; Alkire, R. C., Gerischer, H., Kolb, D. M., Tobias, C. W., Eds.; Wiley-VCH: Weinheim, Germany, 1997; Vol. 5, p 195.
(5) Wilson, M. S.; Gottesfeld, S. *J. Appl. Electrochem.* **1992**, *22*, 1.
(6) Wilson, M. S.; Gottesfeld, S. *J. Electrochem. Soc.* **1992**, *139*, L28.
(7) Li, W.; Ling, C.; Zhou, W.; Qiu, J.; Zhou, Z.; Sun, G.; Xin, Q. *J. Phys. Chem. B* **2003**, *107*, 6292.
(8) Rajesh, B.; Thampi, K. R.; Bonard, J.-M.; Xanthopoulos, N.; Mathieu, H. J.; Viswanathan, B. *J. Phys. Chem. B* **2003**, *107*, 2701.
(9) Yoshitake, T.; Shimakawa, Y.; Kuroshima, S.; Kimura, H.; Ichihashi, T.; Kubo, Y.; Kasuya, D.; Takahashi, K.; Kokai, F.; Yudasaka, M.; Iijima, S. *Physica B* **2002**, *323*, 124.
(10) Steigerwalt, E. S.; Deluga, G. A.; Lukehart, C. M. *J. Phys. Chem. B* **2002**, *106*, 760.
(11) Bessel, C. A.; Laubernds, K.; Rodriguez, N. M.; Baker, R. T. K. *J. Phys. Chem. B* **2001**, *105*, 1115.
(12) Che, G.; Lakshmi, B. B.; Fisher, E. R.; Martin, C. R. *Nature* **1998**, *393*, 346.
(13) Tarasevich, M. R.; Sadkowski, A.; Yeager, E. In *Comprehensive Treatise of Electrochemistry*; Bockris, J. O'M., Conway, B. E., Yeager, E., Khan, S. U. M., White R. E., Eds.; Plenum: New York, 1983; Vol. 7, Chapter 6.
(14) Tanaka, A. A.; Fierro, C.; Scherson, D.; Yeager, E. B. *J. Phys. Chem.* **1987**, *91*, 3799.

10.1021/cm047944y CCC: $30.25
Published on Web 07/26/2005

that the stability of the catalysis in acid electrolytes is improved by pyrolyzing the macrocycles on the support in an inert atmosphere.[15−26] The active site of the heat-treated catalyst has been recognized as the $Fe-N_x$ moiety that remained after the heat treatment and was embedded in the carbon surface.[23−26] A few studies showed that the moiety was also formed by heat treatment of a mixture of Fe salts, carbon black, and an N-containing polymer, such as polypyrrole and polyacrylonitrile.[27,28] These Pt-free catalysts are based on artificially synthesized compounds.

On the other hand, it has been reported oxygen can be reduced at natural organic compounds. Recently, Lai et al. found that an iron enzyme, catalase, immobilized on glassy carbon (GC) electrodes had an activity for O_2 reduction in 0.1 mol dm^{-3} potassium phosphate buffer at pH 8.0.[29] Catalase consists of four equal subunits (molecular weight: 57 000) containing the Fe(III) porphyrin.[30−34] However, the activity was far lower than the conventional Pt/C catalyst, and moreover, the enzyme would be hydrolyzed in the superacidic atmosphere of the polymer electrolyte.[35]

The idea occurred to us that the carbonization of catalase would produce a novel, stable, and active catalyst for O_2 reduction with the active site homogeneously dispersed in a carbon matrix due to the inherent inclusion of the Fe(III) porphyrin. The probability of absence of the moiety on the surface of the carbonized material was one problem of this idea, but it could be overcome by just developing pores inside the material (activation) to expose the moiety to the pore surface. Slow transfer of the O_2 and H^+ in the pores might cause another problem; however, it would also be overcome by CF_3SO_3H adsorption in the pores, since we recently revealed that the effective utilization of the nanospaces in activated carbon loaded with Pt, achieved by the CF_3SO_3H adsorption that enabled fast mass-transfer, produced a highly active catalyst for O_2 reduction in the PEFC.[36]

In this study, we succeeded in the carbonization of catalase and formation of active sites for O_2 reduction. By finely changing the heat-treatment temperature, we found that micropores were highly developed in the carbonized material in a single step simply by carbonization; the activation step was unnecessary. We also found that effectively utilizing the nanospaces by CF_3SO_3H adsorption enhanced the activity for O_2 reduction to produce a sufficiently active catalyst.

Experimental Section

Materials. Catalase from bovine liver was purchased from Sigma and used as received. A commercially available catalyst of 10 wt % platinum on Vulcan XC-72R carbon (Pt/C, ElectroChem) was used as a conventional catalyst. High-purity water was obtained by circulating ion-exchanged water through an Easypure water-purification system (Barnstead, D7403). Perchloric acid (70%, Tama Chemical, analytical grade) was diluted with the high-purity water to prepare 0.1 mol dm^{-3} $HClO_4$. The concentrated perchloric acid was handled with care not to give shocks to it for avoiding its explosion. A solution of Nafion as a perfluorosulfonate ion-exchange resin [equivalent weight (molar mass/mol of ion-exchange site) = 1100, 5 wt % dissolved in a mixture of lower aliphatic alcohols and 15−20% water] was purchased from Aldrich. Nafion 112 was used as the electrolyte membrane for the fuel cell test. The membrane was successively immersed in 3% H_2O_2, the high-purity water, 1 mol dm^{-3} H_2SO_4, and the high-purity water at boiling temperature. After this treatment, the membrane was stored in the high-purity water before use. Potassium trifluoromethanesulfonate (CF_3SO_3K, Tokyo Kasei) was used as received and dissolved in the high-purity water. The argon, hydrogen, and oxygen gases were of ultrahigh purity.

Carbonization of Catalase and Characterization of the Carbonized Materials. The carbonization of catalase was carried out in 0.1 dm^3 min^{-1} of flowing Ar at 700, 750, 800, 850, 900, and 1000 °C for 2 h after raising the temperature at 5 °C min^{-1}. For convenience, the carbonized material produced at 700 °C is hereafter called CC700 and the others in a similar manner. The adsorption isotherm of N_2 onto the carbonized material was measured using an automatic N_2 adsorption apparatus (Belsorp 28, Nihon Bell) at −196 °C. The specific surface area was determined by the Brunauer−Emmet−Teller (BET) plot of the isotherm, and the pore volume by the amount of adsorbed N_2 at the relative pressure of 0.931. The mean pore diameter was calculated by assuming that the pore was cylindrical and using the equation

$$d = 4V_p/S$$

where d is the mean pore diameter, V_p is the pore volume, and S is the specific surface area. The differential pore-volume distributions were also obtained using the isotherm. X-ray photoelectron spectroscopy (XPS) was carried out using a PHI ESCA 5700 system (Physical Electronics) with Al Kα radiation (1486.6 eV), in which the finely ground carbonized material was fixed on an Al adhesive tape. X-ray diffraction (XRD) was performed with an automated RINT 2500 X-ray diffractometer (Rigaku) using Cu Kα radiation. Data acquisition was carried out in the $\theta/2\theta$ step scanning mode at

(15) Widelöv, A.; Larsson, R. *Electrochim. Acta* **1992,** *37*, 187.
(16) Widelöv, A. *Electrochim. Acta* **1993,** *38*, 2493.
(17) Bittins-Cattaneo, B.; Wasmus, S.; Lopez-Mishima, B.; Vielstiech, W. *J. Appl. Electrochem.* **1993**, *23*, 625.
(18) Faubert, G.; Lalande, G.; Côté, R.; Guay, D.; Dodelet, J. P.; Weng, L. T.; Bertrand, P.; Dénès, G. *Electrochim. Acta* **1996**, *41*, 1689.
(19) Lalande, G.; Faubert, G.; Côté, R.; Guay, D.; Dodelet, J. P.; Weng, L. T.; Bertrand, P. *J. Power Sources* **1996**, *61*, 227.
(20) Faubert, G.; Côté, R.; Guay, D.; Dodelet, J. P.; Dénès, G.; Bertrand, P. *Electrochim. Acta* **1998**, *43*, 341.
(21) Bouwkamp-Wijnoltz, A. L.; Visscher, W.; van Veen, J. A. R. *Electrochim. Acta* **1998**, *43*, 3141.
(22) Gojković, S. L.; Gupta, S.; Savinell, R. F. *J. Electroanal. Chem.* **1999**, *462*, 63.
(23) Lefèvre, M.; Dodelet, J. P.; Bertrand, P. *J. Phys. Chem. B* **2000**, *101*, 11238.
(24) Lefèvre, M.; Dodelet, J. P.; Bertrand, P. *J. Phys. Chem. B* **2002**, *106*, 8705.
(25) Lefèvre, M.; Dodelet, J. P. *Electrochim. Acta* **2003**, *48*, 2749.
(26) Schulenburg, H.; Svetoslav, S.; Schünemann, V.; Radnik, J.; Dorbandt, I.; Fiechter, S.; Bogdanoff, P.; Tributsch, H. *J. Phys. Chem. B* **2003**, *107*, 9034.
(27) Gupta, S.; Tryk, D.; Bae, I.; Aldred, W.; Yeager, E. *J. Appl. Electrochem.* **1989**, *19*, 19.
(28) Côté, R.; Lalande, G.; Guay, D.; Dodelet, J. P.; Dénès, G. *J. Electrochem. Soc.* **1998**, *145*, 2411.
(29) Lai, M. E.; Bergel, A. *J. Electroanal. Chem.* **2000**, *494*, 30.
(30) Kiselev, N. A.; Shpitzberg, C. L.; Vainshtein, B. K. *J. Mol. Biol.* **1967**, *25*, 433.
(31) Murthy, M. R. N.; Reid, T. J., III; Sicignano, A.; Tanaka, N.; Rossmann, M. G. *J. Mol. Biol.* **1981**, *152*, 465.
(32) Reid, T. J., III; Murthy, M. R. N.; Sicignano, A.; Tanaka, N.; Musick, W. D. L.; Rossmann, M. G. *Proc. Natl. Acad. Sci. U.S.A.* **1981**, *78*, 4767.
(33) Fita, I.; Rossmann, M. G. *J. Mol. Biol.* **1985**, *185*, 21.
(34) Melik-Adamyan, W. R.; Barynin, V. V.; Vagin, A. A.; Borisov, V. V.; Vainshtein, B. K.; Fita, I.; Murthy, R. N.; Rossmann, M. G. *J. Mol. Biol.* **1986**, *188*, 63.
(35) Samejima, T.; Yang, J. T. *J. Biol. Chem.* **1963**, *238*, 3256.
(36) Maruyama, J.; Abe, I. *J. Electrochem. Soc.* **2004**, *151*, A447.

a speed of 1° min^{-1} with a step size of 0.02° (2θ). A transmission electron micrograph (TEM) was obtained using a JEM-1200EX (JEOL). Mössbauer spectra were recorded at room temperature (FGX-100, Topologic Systems), and α-Fe was used for velocity calibration. Catalase was not enriched by ^{57}Fe for avoiding modification of catalase as a raw material during the enrichment process. Instead, data acquisition was carried out for about 1 month to obtain sufficient counts.[37] Spectra were measured first in a wide isomer shift (δ) range from −10 to 10 mm s^{-1} and then in a narrow range from −2 to 2 mm s^{-1}. Observed spectra were fitted to peaks with a Lorentzian line shape.

Catalyst Layer Formation. The electrochemical characteristics of the carbonized material were fundamentally investigated by fixing it on the surface of a rotating glassy carbon disk electrode (GC RDE) as a catalyst layer and immersing it in 0.1 mol dm^{-3} $HClO_4$.[38−40] An aliquot of 100 mg of the finely ground carbonized material and 10 mg of carbon black (Vulcan XC-72R, Cabot) as the electron-conductive agent were added to 1 mL of the Nafion solution. The mixture was ultrasonically dispersed to produce a catalyst paste. A GC RDE (BAS), which consisted of a GC rod sealed in a Kel-F holder, was polished with a 2000 grit emery paper (Sumitomo 3M) and then ultrasonically cleaned in high-purity water for use as a support for the catalyst layer. The geometric surface area of the electrode was 0.071 cm^2 (diameter, 3 mm). A 1 μL volume of the paste was pipetted onto the GC surface, and to shield it from the irregular air stream generated by a ventilator, the electrode was immediately placed under a glass cover until the layer was formed. After removal of the glass cover, the layer was further dried overnight at room temperature. A catalyst layer was also formed from CC800 with CF_3SO_3H adsorbed in the pores. The adsorption of CF_3SO_3H was carried out by adding 100 mg of CC800 to 5.0 mL of a CF_3SO_3K aqueous solution, and then the mixture was ultrasonically dispersed, followed by centrifuging the mixture and removing the supernatant. We used the potassium salt instead of CF_3SO_3H to avoid handling the superacid for easier operation. After formation of the catalyst layer as described above, K^+ in it was substituted by H^+ by immersing it in 0.1 mol dm^{-3} $HClO_4$. A catalyst layer without the carbonized material was similarly formed from 10 mg of the carbon black and 1 mL of the Nafion solution for comparison. A conventional catalyst layer was also formed from 10 mg of Pt/C and 1 mL of the Nafion solution.

Electrochemical Measurements. An electrochemical analyzer (100B/W, BAS) and an RDE glass cell were used for the cyclic voltammetry and the measurements of the current−potential relationships. The glass cell was cleaned by soaking in a 1:1 mixture of concentrated HNO_3 and H_2SO_4, followed by a thorough rinsing with high-purity water and finally steam-cleaning.[41] The counter electrode was a Pt wire, and the reference electrode was a reversible hydrogen electrode (RHE). All potentials were referred to the RHE. Cyclic voltammograms for the catalyst layers were recorded in Ar-saturated 0.1 mol dm^{-3} $HClO_4$ at 25 °C. The potential was scanned between 0.05 and 1.3 V at a scan rate of 50 mV s^{-1}. Before recording, the potential was repeatedly scanned between 0.05 and 1.4 V to remove any residual impurities. The current−potential relationships were obtained in O_2-saturated 0.1 mol dm^{-3} $HClO_4$ at 25 °C and various rotation speeds. The scan rate of the potential was fixed at 10 mV s^{-1}. Prior to the measurement, the electrode was repeatedly polarized at 0.05 and 1.3 V alternately.[42] The potential was finally stepped to 1.2 V and then swept in the negative direction to obtain a current−potential relationship. The background current was similarly measured in an Ar atmosphere without rotation.

Fuel Cell Tests. A catalyst layer was formed on a 5 cm^2 carbon cloth or paper treated with poly(tetrafluoroethylene) (ElectroChem) as a gas-diffusion layer. A cathode was formed on the carbon cloth from CF_3SO_3H-adsorbed CC800 by spreading the paste similarly prepared as described above with a mixture of the Nafion solution and the high-purity water, drying overnight at room temperature, and substituting K^+ with H^+ by immersing it in 0.1 mol dm^{-3} $HClO_4$. The amounts of CC800, the electron-conductive agent, and Nafion were 10, 1.0, and 5.0 mg cm^{-2}, respectively. An anode was formed using a catalyst paste prepared by adding 50 mg of Pt/C to 2 mL of the mixture of Nafion solution and the high-purity water and ultrasonically dispersing it. The paste was spread on the carbon paper and dried overnight at room temperature. The amounts of Pt/C and Nafion were 1.0 mg cm^{-2} (Pt, 0.1 mg cm^{-2}) and 0.5 mg cm^{-2}, respectively. A cathode for a conventional Pt-based fuel cell for performance comparison was formed on the carbon cloth in the same way. The electrodes and the electrolyte Nafion 112 membrane were pressed at 2.5 MPa and 150 °C for 10 min to form the membrane−electrode assembly, which was then incorporated into a single-cell apparatus (ElectroChem). Hydrogen and oxygen were humidified at 80 °C and passed into the apparatus under atmospheric pressure at 100 cm^3 min^{-1}. The current−potential relationships were measured at 80 °C using a fuel cell station (NF) after a continuous 2-h operation at 0.5 V as a pretreatment. Subsequently, the current at 0.5 V was recorded during a 48-h continuous operation.

Results and Discussion

Development of Nanospace in Carbonized Materials. The heat treatment of catalase at 700, 750, 800, 850, 900, and 1000 °C produced carbonized materials in the following yields: 24.6, 19.6, 14.2, 4.3, 4.6, and 3.1% (the corresponding Fe content calculated from the molecular weight of catalase: 0.40, 0.50, 0.69, 2.3, 2.1, and 3.2%), respectively. The yield decreased with an increase in the heat-treatment temperature.

The pore structures of CC700, CC750, CC800, and CC850 were characterized by the N_2 adsorption isotherms at −196 °C. The heat treatment at above 900 °C shrank the carbonized material which resulted in its hardening and destruction of the porous structure. The specific surface areas and the mean pore diameters determined by the isotherm data were the following: CC700, 290 m^2 g^{-1}, 2.04 nm; CC750, 449 m^2 g^{-1}, 2.04 nm; CC800, 790 m^2 g^{-1}, 2.22 nm; CC850, 975 m^2 g^{-1}, 3.53 nm. The 50 °C difference in temperature caused a significant difference in the pore structure. The surface areas of CC800 and CC850 were as high as that of commercial activated carbon. In addition to these values of specific surface area and mean pore diameter, the differential pore-volume distributions of CC700, CC750, CC800, and CC850 (Figure 1) confirmed a significant development of the nanospaces in the carbonized material. Generally, activated carbon is produced from, for instance, coconut shells or coal

(37) Herod, A. J.; Gibb, T. C.; Herod, A. A.; Xu, B.; Zhang, S.; Kandiyoti, R. *Fuel* **1996**, *75*, 437.
(38) Maruyama, J.; Abe, I. *Electrochim. Acta* **2003**, *48*, 1443.
(39) Gloaguen, F.; Andolfatto, F.; Durand, R.; Ozil, P. *J. Appl. Electrochem.* **1994**, *24*, 863.
(40) Gojković, S. Lj.; Zečević, S. K.; Savinell, R. F. *J. Electrochem. Soc.* **1998**, *145*, 3713.
(41) Chu, D.; Tryk, D.; Gervasio, D.; Yeager, E. B. *J. Electroanal. Chem.* **1989**, *272*, 277.
(42) Razaq, M.; Razaq, A.; Yeager, E.; DesMarteau, D. D.; Singh, S. *J. Electrochem. Soc.* **1989**, *136*, 385.

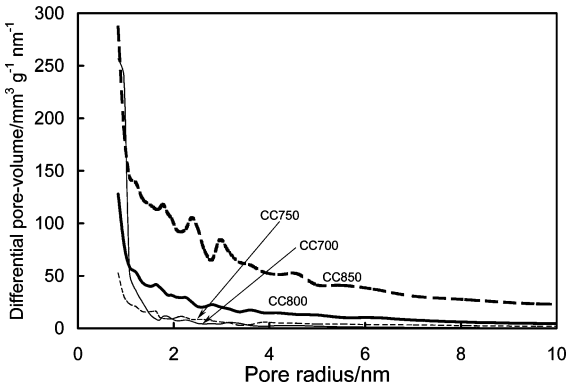

Figure 1. Differential pore-volume distributions of CC700 (thin line), CC750 (thin dashed line), CC800 (thick line), and CC850 (thick dashed line).

through their carbonization and then an activation process using steam, CO_2, or O_2. Without this process, development of pores is insufficient. The specific surface area and the mean pore diameter of charcoal produced from saw dust of Japanese cypress at 800 °C in the same way as the carbonization of catalase were 539 m^2 g^{-1} and 1.83 nm, respectively. In contrast, the results in the present study indicate that activated carbon can be produced from catalase by one procedure with a controlled heat-treatment temperature. At present, however, little is known about carbonized materials from proteins. Recently, we have been investigating the carbonization of proteins in our department using various proteins. The detailed elucidation of the mechanism of the pore forming process is beyond the scope of this study. Further studies are being performed in our department using various proteins to clarify the mechanism which will be reported in another paper.

Active Sites in the Carbonized Material. The surface of the finely ground particles of the carbonized material was analyzed by XPS. The strength of CC850 was low due to excessive pore development leading to failure in obtaining fine particles. Figure 2a shows the X-ray photoelectron spectrum of N 1s in CC800. The peaks at 398.1 and 400.7 eV were attributed to the N atom included in the pyridine- and pyrrole-like surface groups, respectively.[43] These peaks were also observed for CC700 and CC750.

Figure 2b shows the X-ray photoelectron spectrum of Fe $2p_{3/2}$ and $2p_{1/2}$ in CC800. Peaks at 712 eV for Fe $2p_{3/2}$ and 725 eV for Fe $2p_{1/2}$ were observed, although the signal-to-noise ratio for the Fe $2p_{1/2}$ peak was poor even for the most porous materials among CC700, CC750, and CC800, due to the low Fe content. The peak at 712 eV was attributed to Fe(III) according to the value reported in the literature: 710.8−711.8 eV.[44,45] Dodelet et al. and Gojković et al. reported that the peak of Fe $2p_{3/2}$ in heat-treated iron porphyrins adsorbed on carbon black shifted to a lower binding energy due to the formation of aggregates including Fe(0) (706.7−707.2 eV),[44−46] Fe(II) (707.1−708.7 eV),[44,45] or Fe carbides (706.7−706.9 eV)[46,47] with an increase in the heat-treatment temperature.[18−20,48] Gojković also reported a similar peak shift for Fe $2p_{1/2}$ according to the binding energy:[49] Fe(III), 725.1 eV; Fe(II), 722.9 eV; Fe(0), 719.7 eV. Therefore, the results in the present study free of these peak shifts indicated the absence of any aggregates, except for aggregates containing Fe(III) such as Fe_2O_3, which would be possibly formed from Fe and the oxygen of the peptide bonds in the catalase.

However, the absence of the Fe-containing aggregates was also suggested by the XRD spectrum of CC800 shown in Figure 3. The broad peaks at $2\theta = 25$ and 44° were attributed to amorphous carbon,[50] usually observed for activated carbon. Except for the peaks at $2\theta = 21.8$ and 36.2° attributed to SiO_2 present as an impurity derived from the raw material or the porcelain bowl used for the carbonization, which is electrochemically inactive and stable in the polymer electrolyte, there was no peak attributable to the crystalline particles, especially between 40 and 55° where the peaks attributed to the Fe aggregates were reported to appear.[18−20,51−53]

The transmission electron micrographs of CC800 are shown in Figure 4. Amorphous carbon appeared as the gray areas. The dark gray area in Figure 4a was due to the large thickness of the particle, and the black particles in the thinner gray area near the lower left-hand corner of the micrograph were attributed to SiO_2, based on the particle size estimated from the XRD peak. Observation of the carbon part was performed in the thin gray area as shown in Figure 4b,c, suggesting the absence of the Fe aggregates.

Mössbauer spectroscopy was carried out to investigate the chemical environment around Fe. The peaks were observed only in the δ range from −2 to 2 mm s^{-1}. Figure 5 shows the Mössbauer spectrum for CC800 in the δ range from −2 to 2 mm s^{-1}. The peak consisted of three components. The isomer shifts, δ, and quadrupole splittings, Δ, of these components were the following: component A, $\delta = +0.12$ mm s^{-1}, $\Delta = 0.55$ mm s^{-1}; component B, $\delta = +0.38$ mm s^{-1}, $\Delta = 0.40$ mm s^{-1}; component C, $\delta = +0.18$ mm s^{-1}, $\Delta = 0$ mm s^{-1}. The isomer shift and quadrupole splitting of component A was close to those of the Mössbauer spectrum of hematin.[54] The components B and C were similar to the peaks observed for Fe protoporphyrin IX dimers and oligomers.[55] The spectrum in Figure 5 was, therefore, attributable to porphyrin-like structures surrounding Fe in CC800. This interpretation was supported by previous studies in which it

(43) Casanovas, J.; Ricart, J. M.; Rubio, J.; Illas, F.; Jiménez-Mateos, J. M. *J. Am. Chem. Soc.* **1996**, *118*, 8071.
(44) Johansson, L. Y.; Larsson, R. *Chem. Phys. Lett.* **1974**, *24*, 508.
(45) Choudhury, T.; Saied, S. O.; Sullivan, J. L.; Abbot, A. M. *J. Phys. D: Appl. Phys.* **1989**, *22*, 1185.
(46) Sethuraman, R.; Stencel, J. M.; Rubel, A. M.; Cavin, B.; Hubbard, C. R. *J. Vac. Sci. Technol., A* **1994**, *12*, 443.
(47) Schwar, J.; Jahn, P. W.; Wiedmann, L.; Benninghoven, A. *J. Vac. Sci. Technol., A* **1991**, *9*, 238.
(48) Gojković, S. L.; Gupta, S.; Savinell, R. F. *J. Electrochem. Soc.* **1998**, *145*, 3493.
(49) Mills, P.; Sullivan, J. L. *J. Phys. D: Appl. Phys.* **1983**, *16*, 723.
(50) Bron, M.; Radnik, J.; Fieber-Erdmann, M.; Bogdanoff, P.; Fiechter, S. *J. Electroanal. Chem.* **2002**, *535*, 113.
(51) Faubert, G.; Côté, R.; Dodelet, J. P.; Lefèvre, M.; Bertrand, P. *Electrochim. Acta* **1999**, *44*, 2589.
(52) Lalande, G.; Côté, R.; Guay, D.; Dodelet, J. P.; Weng, L. T.; Bertrand, P. *Electrochim. Acta* **1997**, *42*, 1379.
(53) Faubert, G.; Côté, R.; Guay, D.; Dodelet, J. P.; Dénès, G.; Poleunis, C.; Bertrand, P. *Electrochim. Acta* **1998**, *43*, 1969.
(54) Karger, W. *Ber. Bunsen-Ges. Phys. Chem.* **1964**, *68*, 793.
(55) Burda, K.; Hrynkiewicz, A.; Kołoczek, H.; Stanek, J.; Strzałka, K. *Biochim. Biophys. Acta* **1995**, *1244*, 345.

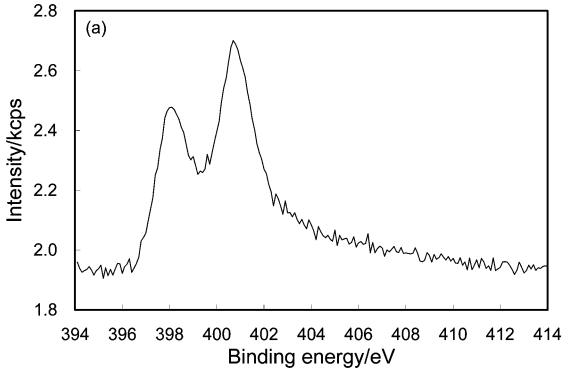

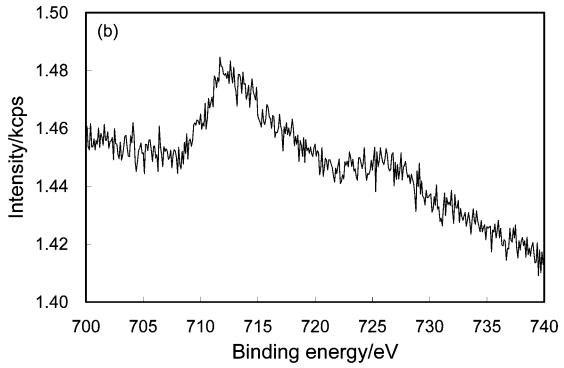

Figure 2. X-ray photoelectron spectra of N 1s (a) and Fe 2p (b) in CC800.

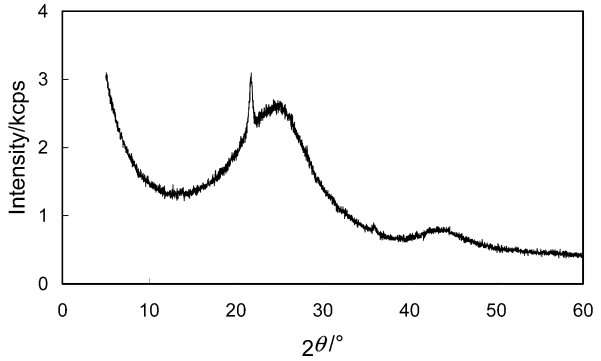

Figure 3. X-ray diffraction spectrum of CC800.

was shown that the porphyrin-like structures was retained in carboneous compounds after the pyrolysis of their precursor containing metal porphyrins, based on the analysis using XPS,[15] X-ray adsorption near-edge structure spectroscopy,[56] and Mössbauer spectroscopy.[37]

The results of XPS, XRD, TEM, and Mössbauer spectroscopy in this study suggested that Fe(III) was finely dispersed and coordinated by four N atoms which originated from the porphyrin in catalase.

Cyclic Voltammetry. Figure 6 shows the cyclic voltammograms for the catalyst layers in Ar-saturated 0.1 mol dm^{-3} $HClO_4$, which provides information on the electrochemical surface properties of the carbonized materials in contact with the polymer electrolyte. The sign of the current due to the oxidation reactions was taken as positive, and that due to the reduction reaction was taken as negative. The current in both the positive and negative scan increased with an increase in the heat-treatment temperature. Charging of the electrochemical double layer might mostly cause the current due to the large surface area of the carbonized material. The increase in the current was in agreement with the increase in the surface area. Very broad peaks situated at 0. 65 V in the positive scan and 0.40 V in the negative scan for the CC800 layer free of CF_3SO_3H were attributable to the redox reaction of quinone-like functional groups (Q) on the surface of CC800, which are usually observed for carbon electrodes:[57]

$$Q + 2H^+ + 2e^- \leftrightarrow QH_2 \qquad (3)$$

A broad peak at 0.55 V in the positive scan for the CC750 layer was also attributable to the oxidation of the surface functional group, although its reduction peak was not observed. Since the reduction requires proton transfer inside the pores, the absence of the peak was probably due to the large overpotential caused by restriction of the H^+ transfer in the insufficiently developed pores with the minute pore diameter in CC750. For the CC700 layer, the low surface area limited the number of functional groups that resulted in almost eliminating the peaks. In the cyclic voltammogram for the CF_3SO_3H-adsorbed CC800 layer, the current in both the positive and negative scans decreased, compared to the CF_3SO_3H-free CC800 layer, due to surface blocking by CF_3SO_3H. In addition, the peak potential for the reduction of Q at the former layer was slightly higher than that at the latter layer. This was attributable to the improved H^+ transfer due to the presence of CF_3SO_3H. Since the large surface area of activated carbon is generally derived from the micropores, the current in the voltammograms was generated mainly at the surface of the micropores. This result indicated that the presence of CF_3SO_3H in the nanospaces of CC800. Although the hydration state of CF_3SO_3H in the micropores would be different from that in the bulk solution and is not clear at present,[58] it could be assumed from the studies by Zawodzinski et al.[59,60] that the size of hydrated CF_3SO_3H is approximately $0.5 \times 0.5 \times 0.5$ nm. The hydrated CF_3SO_3H is sufficiently small to be present in the nanospaces.

In all the voltammograms, there was no peak attributed to Fe dissolution, which was observed for the heat-treated Fe porphyrin adsorbed on carbon black,[48] although long-term Fe retention could not be confirmed. In addition, no peaks were observed for the Fe(III)/Fe(II) redox couple that should be associated with oxygen reduction. A similar behavior was recently reported by Bouwkamp-Wijnoltz et al.[61] They attributed the absence of the peak to the broad distribution of the redox potential or to the slow electron-transfer rate. The same situation might also occur for the carbonized material in this study.

(56) Jones, J. M.; Zhu, Q.; Thomas, K. M. *Carbon* **1999**, *37*, 1123.
(57) Maruyama, J.; Abe, I. *Electrochim. Acta* **2001**, *46*, 3381.
(58) Ohkubo, T.; Konishi, T.; Hattori, Y.; Kanoh, H.; Fujikawa, T.; Kaneko, K. *J. Am. Chem. Soc.* **2002**, *124*, 11860.
(59) Paddison, S. J.; Zawodzinski, T. A., Jr. *Solid State Ionics* **1998**, *113*−*115*, 333.
(60) Eikerling, M.; Paddison, S. J.; Pratt, L. R.; Zawodzinski, T. A., Jr. *Chem. Phys. Lett.* **2003**, *368*, 108.
(61) Bouwkamp-Wijnoltz, A. L.; Visscher, W.; van Veen, J. A. R.; Boellaard, E.; van der Kraan, A. M.; Tang S. C. *J. Phys. Chem. B* **2002**, *106*, 12993.

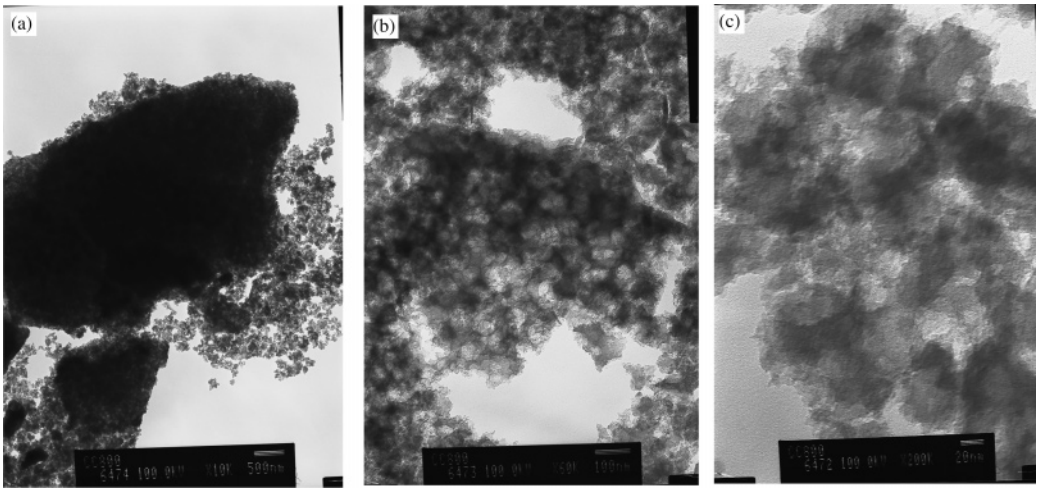

Figure 4. Transmission electron micrographs of CC800. The acceleration voltage was 100.0 kV. The scale bars in the micrograph correspond to (a) 500 nm, (b) 100 nm, and (c) 20 nm.

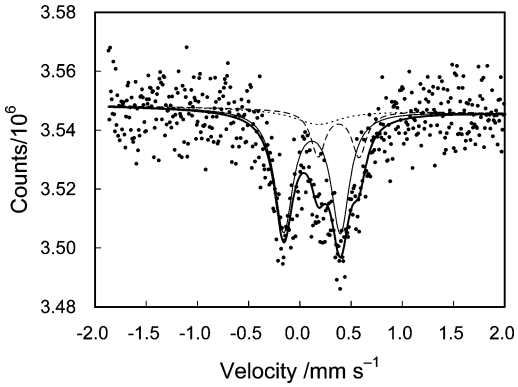

Figure 5. Mössbauer spectrum of CC800 at room temperature: observed (●) and calculated spectra (thick line) consisting of component A (thin line), component B (thin dashed line), and component C (thin dotted line).

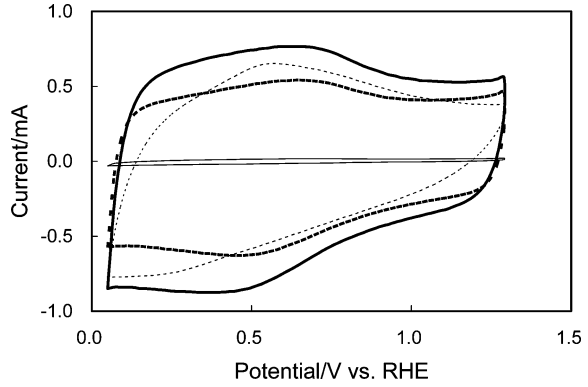

Figure 6. Cyclic voltammograms for catalyst layers formed from CC700 (thin line), CC750 (thin dashed line), CC800 (thick line), and CF_3SO_3H-adsorbed CC800 (thick dashed line) in Ar-saturated 0.1 mol dm^{-3} $HClO_4$ at 25 °C. Scan rate: 50 mV s^{-1}. The concentration of CF_3SO_3K solution used for adsorption onto CC800 was 0.5 mol dm^{-3}.

Oxygen Reduction. Oxygen reduction currents at the catalyst layers were measured in O_2-sarturated 0.1 mol dm^{-3} $HClO_4$ with the electrodes rotated at various rotation speeds. Figure 7 shows the relationships between the electrode potential and currents at the catalyst layers formed from CC700, CC750, CC800, CF_3SO_3H-adsorbed CC800, only an electron-conductive agent, and Pt/C, measured by rotating the electrodes at 2000 rpm. The current shown in Figure 7 was obtained by subtracting the background current from the measured current. The O_2 reduction currents at the

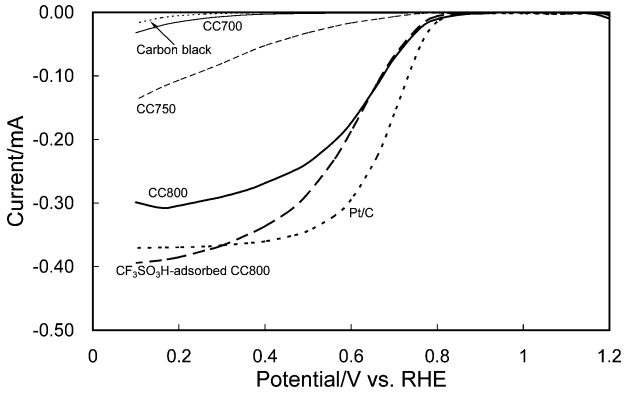

Figure 7. Relationships between electrode potential and oxygen reduction current of negative scans at catalyst layers formed from CC700 (thin line), CC750 (thin dashed line), CC800 (thick line), CF_3SO_3H-adsorbed CC800 (thick dashed line), carbon black (thin dotted line), and Pt/C (thick dotted line) in O_2-saturated 0.1 mol dm^{-3} $HClO_4$ at 25 °C. Scan rate: 10 mV s^{-1}. Electrode rotation speed: 2000 rpm. The concentration of CF_3SO_3K solution used for adsorption onto CC800 was 0.5 mol dm^{-3}.

catalyst layers formed from the carbonized material were greater than that at the layer without it and increased with an increase in the heat-treatment temperature. Adsorption of CF_3SO_3H in the pores of CC800 further increased the current below 0.6 V. When the concentration of the CF_3SO_3K solution used in the adsorption procedure was 0.5 mol dm^{-3}, the highest current was obtained. The results of the CF_3SO_3H-adsorbed CC800 layer shown hereafter were for that formed using 0.5 mol dm^{-3} CF_3SO_3K. The current below 0.3 V was greater than that at the conventional Pt/C catalyst layer containing Pt whose weight was nearly equal to that of Fe in the CF_3SO_3H-adsorbed CC800 layer. These currents shown in Figure 7 arose from the O_2 reduction inside the catalyst layer but included the influence of the mass-transfer in the 0.1 M $HClO_4$ solution in which the catalyst layer was immersed. The activities of the catalyst layers for O_2 reduction were evaluated using the reduction current free of the influence of the mass transfer in the solution, I_K, determined by the equation[38]

$$-\frac{1}{I} = -\frac{1}{I_K} + \frac{1}{0.620nFAD^{2/3}c\nu^{-1/6}\omega^{1/2}}$$

where I is the reduction current after subtracting the

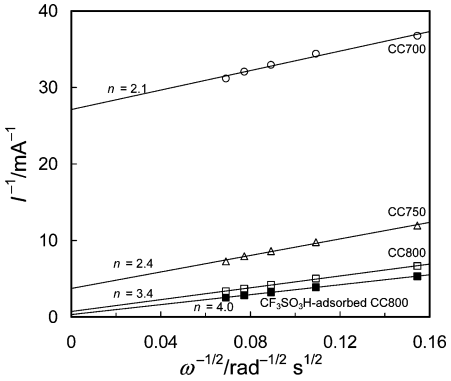

Figure 8. $-1/I$ vs $\omega^{-1/2}$ plots for oxygen reduction and number of electrons involved in the reaction per molecule at 0.1 V for catalyst layers formed from CC700 (○), CC750 (△), CC800 (□), and CF_3SO_3H-adsorbed CC800 (■).

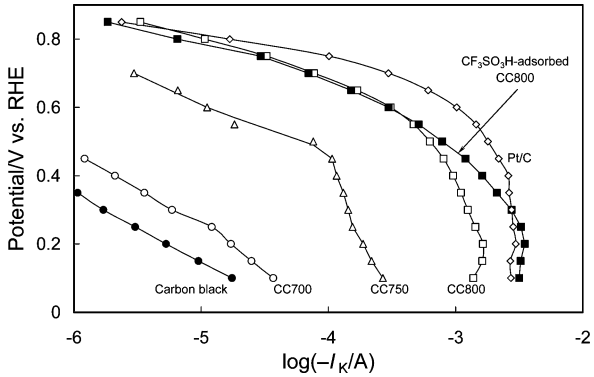

Figure 9. Relationships between electrode potential and $\log(-I_K/A)$ for catalyst layers formed from CC700 (○), CC750 (△), CC800 (□), and CF_3SO_3H-adsorbed CC800 (■). Relationships for catalyst layers formed from carbon black (●) and that formed from Pt/C (◇) are also shown for comparison. Fe loading on GC RDE: CC700 layer, 0.40 μg; CC750 layer, 0.50 μg; CC800 and CF_3SO_3H-adsorbed CC800 layer, 0.69 μg. Pt loading on GC RDE: 1 μg.

background current, n is the number of electrons involved in the O_2 reduction/molecule, F is the Faraday constant, A is the geometric area of the GC electrode, D is the diffusion coefficient of O_2 in solution, c is the concentration of O_2 in solution, ν is the kinematic viscosity of the solution, and ω is the angular frequency of rotation. Figure 8 shows $-1/I$ vs $w^{-1/2}$ plots for the O_2 reduction at 0.1 V and n that were calculated using the slope of the plot and the following values:[62−64] F, 96485 C mol^{-1}; A, 0.0707 cm^2; D, 1.9×10^{-5} cm^2 s^{-1}; c, 1.18×10^{-6} mol cm^{-3}; ν, 9.87×10^{-3} cm^2 s^{-1}. A two-electron reduction generates the intermediate H_2O_2 (reaction 4). An increase in n occurs with its further reduction (reaction 5), the decomposition of H_2O_2 (reaction 6), or increase in the proportion of the four-electron reduction to H_2O (reaction 2).[65]

$$O_2 + 2H^+ + 2e^- \rightarrow H_2O_2 \quad (4)$$

$$H_2O_2 + 2H^+ + 2e^- \rightarrow 2H_2O_2 \quad (5)$$

$$2H_2O_2 \rightarrow 2H_2O + O_2 \quad (6)$$

At the CC700 layer, n was 2.1, indicating that the two-electron reduction predominated and the oxygen reduction occurred mainly on the carbon surface.[13] The number of electrons increased with an increase in the heat-treatment temperature: 2.4 at the CC750 layer; 3.4 at the CC800 layer. The development of micropores exposed the active sites in the carbonized material that resulted in the increase. The adsorption of CF_3SO_3H in the pores of CC800 achieved an increase in n to 4, indicating that the CF_3SO_3H-adsorbed CC800 layer was capable of directly reducing O_2 to H_2O without releasing H_2O_2, which would damage the active site and the polymer electrolyte.[25,26] The increase was explained by the expansion of the electrochemically active area for O_2 reduction to deep inside the pores, due to the fast mass-transfer by CF_3SO_3H; the H_2O_2 generated there could be further reduced (reaction 5) or decomposed (reaction 6) during its transfer to the outside of the pores. Investigating the reaction routes and dependence of n and the H_2O_2 generation on the electrode potential in detail would require further studies using other electrochemical instrumentation, such as a rotating ring-disk electrode system.

The relationships between the electrode potential and $\log(-I_K/A)$ (Tafel plots) are shown in Figure 9. The amounts of Fe loaded on GC RDE were the folowing: the CC700 layer, 0.40 μg; the CC750 layer, 0.50 μg; the CC800 and CF_3SO_3H-adsorbed CC800 layer, 0.69 μg. The amount of Pt loaded on GC RDE was 1 μg. The activity for O_2 reduction at the catalyst layers formed from the carbonized material was significantly greater than that at the layer formed only from carbon black and increased with an increase in the heat-treatment temperature. The increase in the activity was far beyond the increase in the amount of Fe in the catalyst layer. Thus, the increase in the number of active sites caused by the development of micropores could essentially produce the increase in $-I_K$. In addition, the heat-treatment at 800 °C would produce the catalyst with maximum activity, according to previous studies.[18,19,22−25] The combination of these two effects substantially changed $-I_K$ with only a 50 °C change in the heat-treatment temperature.

The adsorption of CF_3SO_3H in the pores of CC800 achieved a further increase in $-I_K$, attributed to the fast mass-transfer in the pores. Although the largest difference in $-I_K$ between the CF_3SO_3H-adsorbed CC800 layer and the Pt/C layer was observed at 0.7 V, $-I_K$ at the former was approximately 1/4 small than that at the latter; the difference was in the range of 1 order of magnitude, and below 0.3 V, $-I_K$ at the former was greater than that at the latter. Therefore, one might be able to conclude that the activity of the CF_3SO_3H-adsorbed CC800 layer was comparable to the conventional Pt/C layer. A slight decrease was observed compared to the CF_3SO_3H-free CC800 layer in the high potential region where the O_2 reduction current was low, diminishing the effect of fast mass transfer. The decrease was due to the surface blocking by CF_3SO_3H as confirmed in the cyclic voltammograms. However, the effect of fast mass transfer obviously predominated considering the whole potential range. This activity increase indicated that the active

(62) Maruyama, J.; Abe, I. *J. Electroanal. Chem.* **2003**, *545*, 109.
(63) Zečević, S. K.; Wainright, J. S.; Litt, M. H.; Gojković, S. Lj.; Savinell, R. F. *J. Electrochem. Soc.* **1997**, *144*, 2973.
(64) Mello, R. M. Q.; Ticianelli, E. A. *Electrochim. Acta* **1997**, *42*, 1031.
(65) Maruyama, J.; Inaba, M.; Morita, T.; Ogumi, Z. *J. Electroanal. Chem.* **2001**, *504*, 208.

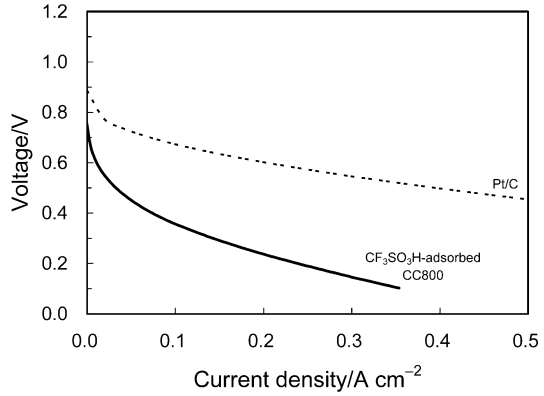

Figure 10. Relationships between cell voltage and currents generated by fuel cells formed from CF_3SO_3H-adsorbed CC800 (solid line) and Pt/C (dotted line). Catalyst loading: CC800, 10 mg cm^{-2} (Fe, 0.069 mg cm^{-2}); Pt/C, 1 mg cm^{-2} (Pt, 0.1 mg cm^{-2}). Cell temperature: 80 °C. Hydrogen and oxygen were humidified at 80 °C and passed into the cell apparatus at 100 cm^3 min^{-1} and atmospheric pressure.

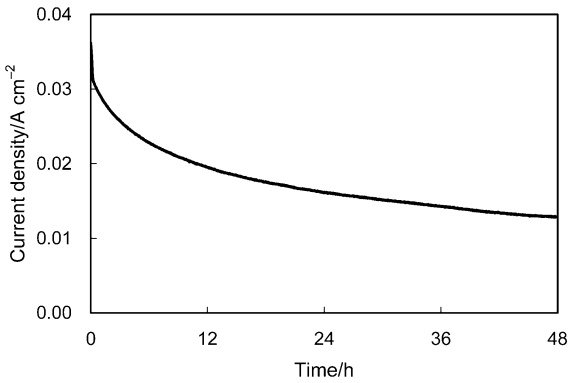

Figure 11. Current change in a fuel cell formed from CF_3SO_3H-adsorbed CC800 during continuous operation at 0.5 V. Cell temperature: 80 °C. Hydrogen and oxygen were humidified at 80 °C and passed into the cell apparatus at 100 cm^3 min^{-1} and atmospheric pressure.

sites which were situated deep inside of the pores functioned effectively. Therefore, the result implied the homogeneous distribution of the active sites in the carbonized materials. The adsorption of CF_3SO_3H in the pores enabled the effective utilization of the nanospaces of the carbonized material.

Fuel Cell Test. Preliminary fuel cell tests were carried out by forming cathodes from the CF_3SO_3H-adsorbed CC800 layer and a Pt/C layer containing Pt whose weight was nearly equivalent to that of Fe in the former layer. Figure 10 shows the relationships between the cell potential and the currents generated by the fuel cells. The performance of the conventional Pt/C fuel cell was nearly equivalent to that previously reported, considering the Pt loading.[66] The results confirmed that the single cell formed from the carbonized material generated electricity, although the performance was inferior to that of the conventional fuel cell. The performance decreased during continuous operation at 0.5 V (Figure 11); the current significantly decreased during the first 24 h, 45% of the initial current, and gradually decreased to 36% at 48 h. It should be noted that the parameters for the cathode catalyst layer formation were not optimized. The parameters are, for instance, particle size of the carbonized material and composition: the amounts of the carbonized material, the electron-conductive agent, and the polymer electrolyte. Modification of the carbonizing conditions, such as the atmosphere and heating rate, would also improve the activity and durability. Further studies are required and are currently underway.

Conclusions

An active Pt-free catalyst for O_2 reduction, which functions in a superacidic atmosphere, was produced by carbonizing a natural organic compound, catalase. The carbonized material possessed highly developed micropores that could be effectively utilized by the adsorption of CF_3SO_3H, which imparted an activity for O_2 reduction comparable to a conventional Pt/C catalyst and the ability to reduce O_2 directly to H_2O. The active site in the carbonized material was Fe(III) coordinated by four N atoms that originated from porphyrin in catalase. The sites were finely and homogeneously dispersed in the material and exposed to the surface by the development of micropores. The nanospaces were developed under strict conditions, but in a single step, by simply heat-treating in an inert atmosphere. Conventionally, catalysts have been generally produced in two steps, i.e., production of a support and loading of active materials, such as Pt and organic macrocycles coordinating Fe, on the support. In contrast, the carbonization of catalase simultaneously produced the active sites and a carbon matrix as the support of the active sites.

A preliminary fuel cell test confirmed that the carbonized material could be used in the cathode to generate electricity, although the performance was inferior to that of a conventional Pt/C fuel cell. The activity and stability will be further improved by optimization of the carbonization condition, and a method for the catalyst layer formation is also necessary. At present, the material cost for CC800 was nearly equivalent to that for the catalysts formed from the organic macrocycles but higher than that of Pt/C; however, the cost can be reduced by the development of easy methods for the extraction of catalase from cells and its production, due to advanced biotechnology, because catalase is present in almost all aerobically respiring organisms, protecting the cells from the toxic effects of H_2O_2.[67]

It should be noted that the PEFC anode still requires Pt or Pt alloys as a catalyst. However, there is room for reducing its amount due to high reaction rate of H_2 oxidation compared to O_2 reduction.[68,69] This study demonstrated a way to significantly reduce the total amount of Pt used in the PEFC.

Acknowledgment. We thank Dr. M. Chigane for his help with the XPS measurements and Dr. M. Yamamoto and Mr. T. Sinagawa for their help with the XRD measurements. We also thank Dr. H. Yamanaka for discussions on the enzymes. We also thank Dr. H. Sakaebe for the Mössbauer measurements, Dr. T. Abe for discussions on the state of Fe in the carbonized materials, and Dr. J. Ozaki for discussions on thermal decomposition of porphyrins.

CM047944Y

(66) Gamburzev, S.; Appleby, A. J. *J. Power Sources* **2002**, *107*, 5.

(67) Chance, B.; Sies, H.; Boveris, A. *Physiol. Rev.* **1979**, *59*, 527.

(68) Gasteiger, H. A.; Panels, J. E.; Yan, S. G. *J. Power Sources* **2004**, *127*, 162.

(69) Wang, J. X.; Brankovic, S. R.; Zhu, J. C.; Hanson, J. C.; Adžić, R. R. *J. Electrochem. Soc.* **2003**, *150*, A1108.